Supplementary Information

Zinc Oxide Nanoclusters Encapsulated in MFI Zeolite as a Highly Stable Adsorbent for the Ultradeep Removal of Hydrogen Sulfide

*Tao Yu, Jinyu Zheng, Shikun Su, Yundong Wang, * Jianhong Xu* and Zhendong Liu**

Correspondence: wangyd@tsinghua.edu.cn (Y.W.)

xujianhong@tsinghua.edu.cn (J.X.)

liuzd@tsinghua.edu.cn (Z.L.)

Table of content

Experimental section

Materials. Tetrapropylammonium hydroxide (TPAOH, KENTE catalysts Inc., 40 wt%), tetraethoxysilane (TEOS, Aldrich, 98%) and zinc nitrate hexahydrate ($Zn(NO)_3 \cdot 6H_2O$, Aladdin, 99.99%) were purchased and used in this work. And distilled water produced in laboratory. All the chemicals were commercially available and were used without any further purification.

Synthesis of silicalite-1. A certain amount of TPAOH was mixed with distilled water in a polypropylene bottle at first, followed by the addition of TEOS, yielding a precursor with the following molar composition, 1 SiO_2 : 4EtOH : 0.25 TPAOH : 20 H_2O. After 15 min of vigorous stirring at 400 rpm, the mixture was charged into Teflon-lined autoclave and placed in an air-circulated oven at 443 K under tumbling condition (40rpm). The obtained solid phase was centrifuged, washed with distilled water until a neutral pH was attained, then dried at 353 K overnight. Finally, the dried solid was calcined at 823 K for 7 h. The temperature of 823 K was attained with a heating rate of 2 K/min.

Synthesis of hollow silicalite-1 (Hol-S-1). Hol-S-1 was synthesized from S-1. A mixture of S-1 and TPAOH with a composition of 1 S-1 : 0.1 TPAOH : 55 H_2O were mixed in a polypropylene bottle under vigorous stirring at 400 rpm for 15 min, then the mixture was transferred into Teflon-lined autoclave and placed in an air-circulated oven at 443 K under tumbling condition (60rpm). The obtained solid phase was centrifuged, washed with distilled water until a neutral pH was attained, then dried at 353 K

overnight. Finally, the dried solid was calcined at 823 K for 7 h. The temperature of 823 K was attained with a heating rate of 2 K/min.

Synthesis of ZnO@S-1 and ZnO@Hol-S-1. ZnO@S-1 and ZnO@Hol-S-1 adsorbents with different ZnO ratios were prepared by traditional impregnation method. At first, a required amount of $Zn(NO)_3 \cdot 6H_2O$ was dissolved in 5 mL distilled water, then the 1 g of zeolite powder was added to the above solution. The obtained impregnation solution was ultrasonicated for 30 min, then was left stand still for 3 h, followed by drying at 353 K overnight and calcination at 623 K for 6 h. The final samples were denoted as *x* wt% ZnO@S-1, Hol-S-1 or nano-S-1, where *x* represented the number of weight percent (wt%) of ZnO.

Characterization. XRD patterns were collected by a Bruker D8 advance with Cu Kα radiation at a scanning speed of 5 $^{o}min^{-1}$ in the 2theta range of 5-50^{o}. ICP-OES methodology was carried out to determine Zn content in the samples. All the samples were digested with hydrofluoric acid and nitric acid before analyzed on Thermo Scientific iCAP 7400 duo optical emission spectrometer fitted with a simultaneous charge induction detector. SEM images were acquired using a Hitachi SU8010 microscope.High-angle annular dark field scanning transmission electron microscopy (HAADF-STEM) with the elemental mapping and high-resolution transmission electron microscope (HRTEM) were acquired using a JEOL JEM-2100F microscope operating at 200 kV. Nitrogen adsorption-desorption isotherms were determined by auto surface area & pore size analyzer (Quadrasorb SI) at liquid nitrogen temperature (77K). Brunauer-Emmett-Teller (BET) and t-plot method were used to calculate the

surface area and micropore volume, respectively.The XPS measurements were conducted on a Thermo Fisher ESCALAB 250Xi device with an Al Kα radiation source. The binding energy was calibrated by C 1s at 284.8 eV. The DRIFT spectra was recorded on a Nicolet 6700. The samples were required to be heated to 723 K under nitrogen atmosphere and maintained for more than 4 hours to exclude the effect of water before characterization. The UV-vis spectra were recorded on Agilent Cary 5000 Scan UV-vis spectrophotometer equipped with an integration sphere. All the measurements were carried out in air at room temperature. XAS spectra was collected at the 1W1B beam line in the Beijing Synchrotron Radiation Facility (BSRF). The extended X-ray absorption fine structure (EXAFS) spectra were obtained by using a standard procedure of data reduction and least-squares fitting following the IFEFFIT code; the phase and amplitude function were analyzed using the FEFF 9.0 code [1]. ^{1}H MAS NMR measurements were performed on a JNM-ECZ600R spectrometer equipped with a 14.09 T wide-bore magnet at a resonance frequency of 600 MHz. Prior to NMR measurement, all the samples were dehydrated in stainless steel tube on a vacuum system for 15 h under heating at 673 K. A 3.2 mm outer diameter zirconia rotor was used and ca. 40 mg of samples was loaded in a typical measurement.

Adsorption test. Adsorption tests were carried out at 150 °C to determine the breakthrough capacity and stability of adsorbents for H_2S removal. Figure S1 shows the diagram of the device. Adsorbent samples (ca. 50 mg) were evaluated in a continuous-flow fixed-bed glass microreactor (i.d. = 6 mm). Prior to the experiments run, samples were activated in He flow for 4 h at 623 K. He containing 10 ppm H_2S

was then passed through column of adsorbent at 50 mL/min. The breakthrough of H_2S was monitored using a gas chromatograph (Huaai, GC-9560) equipped with a flame photometric detector (FPD). The fixed bed was considered as breakthrough when the outlet concentration reached 2 ppm. After sulfidation, the gas flow was switched to nitrogen containing 5% oxygen at 773 K and maintained for 4 h to perform regeneration procedure. The regenerated sample was again evaluated for H_2S removal under the same experimental condition as for fresh samples. The breakthrough capacities (BSC) and ZnO utilization were calculated according to the following equations.

$$BSC = \frac{\mathrm{v} \times \int_0^t (C_{in} - C_{out})\, dt \times M \times 10^{-4}}{V_{mol} \times m_s}$$

v - flow rate, L/min;

t - breakthrough time, min;

C_{in}, C_{out} - inlet, outlet H_2S concentration, ppm;

M - molar mass of sulfur, g/mol;

V_{mol} - molar volume of gas at experimental temperature, L/mol;

m_s - weight of adsorbent, g;

$$utilizaiton = \frac{\mathrm{BSC} \times M_z \times 10^{-3}}{\mathrm{M} \times \mathrm{x}}$$

M_z - molar mass of zinc oxide, g/mol;

M - molar mass of sulfur, g/mol;

x - zinc oxide content in adsorbent;

Table S1 Micropore and total volume data of silicalite-1 and ZnO@silicalite-1 with different ZnO loadings

	S-1	1% ZnO@S-1	2% ZnO@S-1	5% ZnO@S-1
V_{mic} (cm^3/g) [a]	0.161	0.159	0.149	0.115

[a] V_{mic} is calculated by *t*-plot method.

Table S2 Peak assignments of the ^1H NMR spectra of the MFI zeolite

chemical shift/ ppm	assignment
1.05 – 2.1	Isolated [2,3]/geminal [4]/internal [5] silanols
2.6 – 4.6	medium H-bonding silanols [6] H-bonding water [4]
4.8 – 8.4	silanol nests [6] bridging SiOHAl [7] strong H-bonding silanols [6]

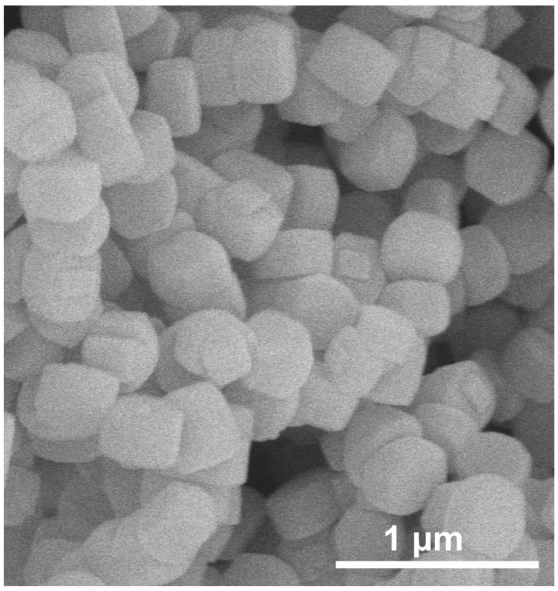

Figure S1 SEM image of silicalite-1

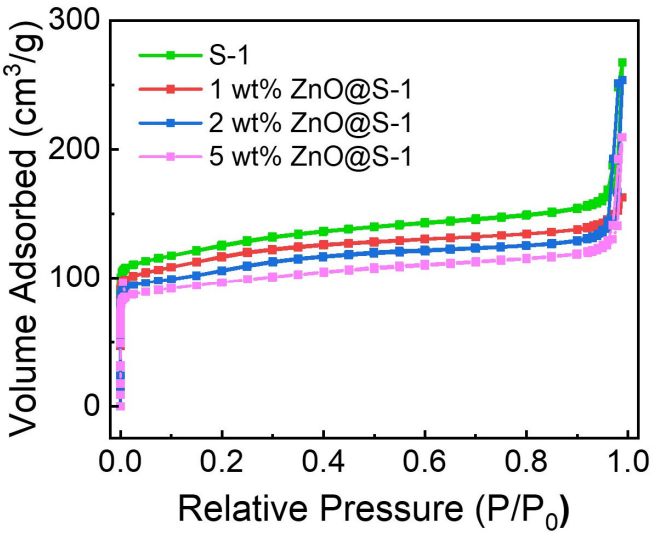

Figure S2 N_2 adsorption-desorption of silicalite-1 and ZnO@silicalite-1 with different ZnO loadings

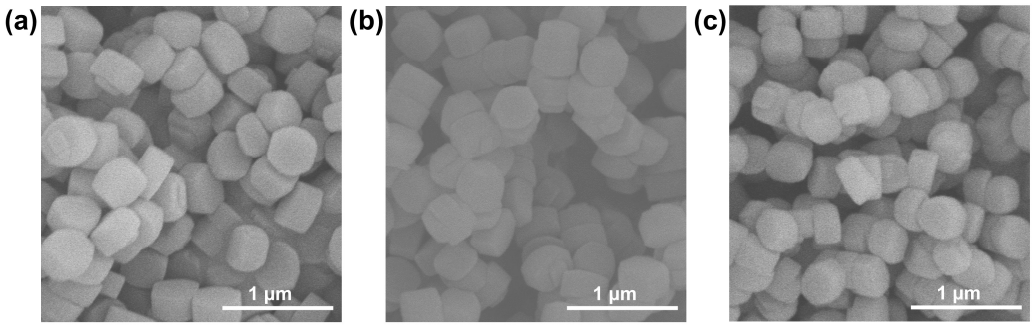

Figure S3 Morphology of ZnO@silicalite-1 with different ZnO loadings.
(a) SEM images of 1wt% ZnO@silicalite-1. (b) SEM images 2 wt% ZnO@silicalite-1 and (c) SEM images 5 wt% ZnO@silicalite-1.

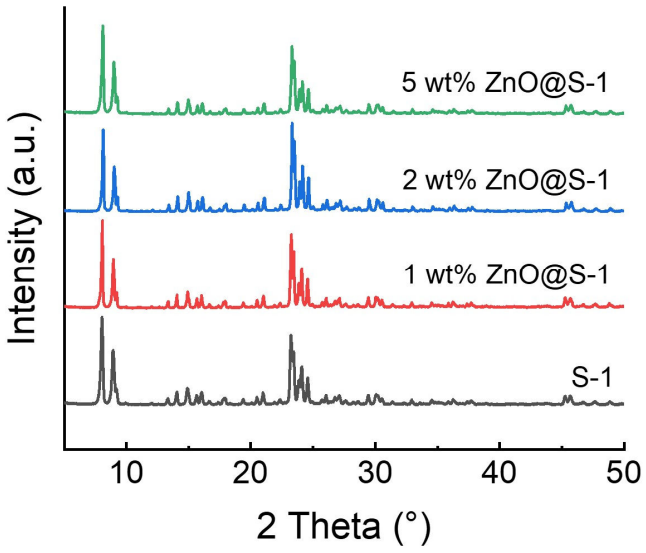

Figure S4 XRD patterns of silicalite-1 and ZnO@silicalite-1 with different ZnO loadings.
(note: ZnO@S-1 represents ZnO@silicalite-1)

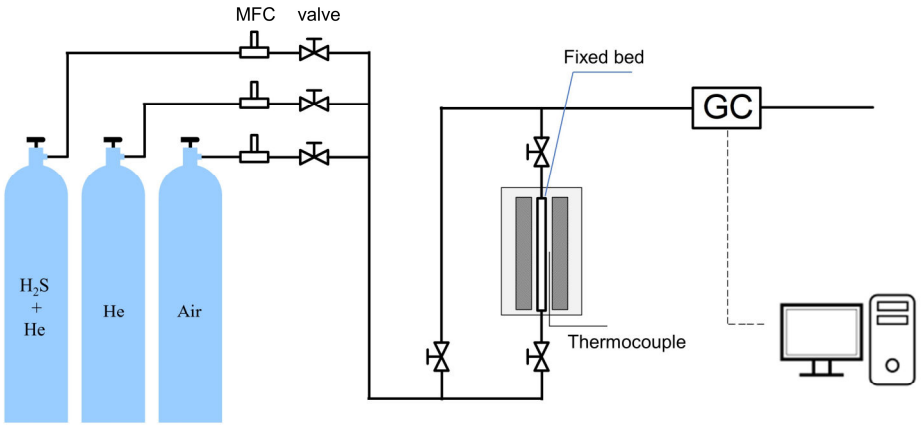

Figure S5 Diagram of adsorption test device.

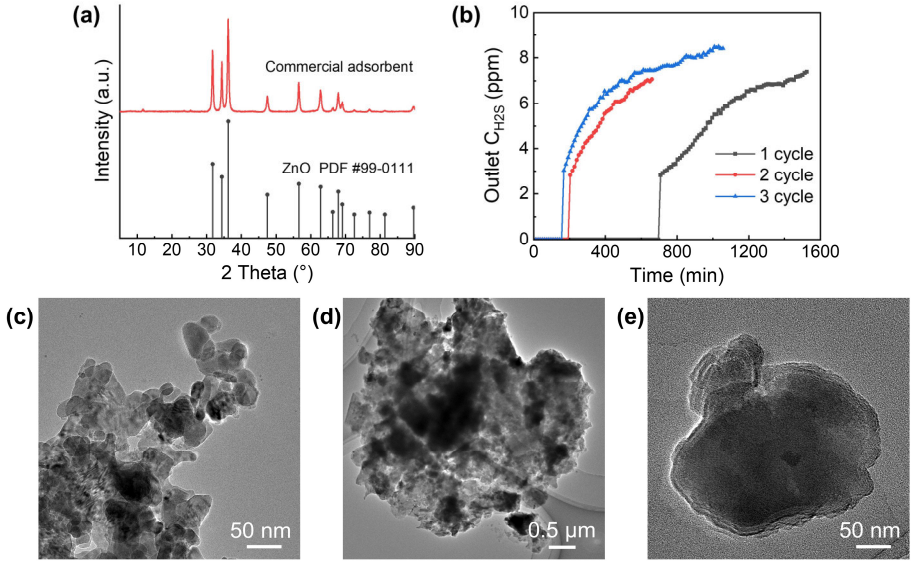

Figure S6 Evolution of commercial ZnO adsorbent during sulfidation and regeneration.

(a) XRD pattern of commercial adsorbent and standard XRD pattern of ZnO; (b) Breakthrough curve of commercial H_2S adsorbent; (c) HRTEM image of the fresh ZnO nanoparticles. (d) and (e) HRTEM images of the regenerated ZnO nanoparticles after the regeneration in air at 500 °C for 6 h.

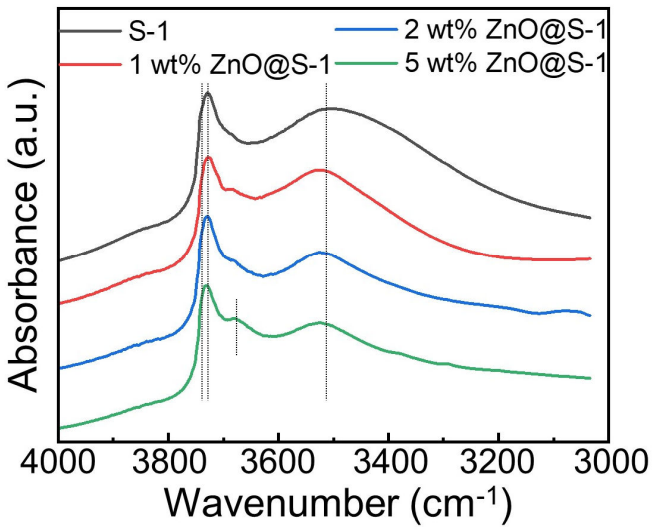

Figure S7 DRIFT spectra of ZnO@silicalite-1 with different ZnO loadings.

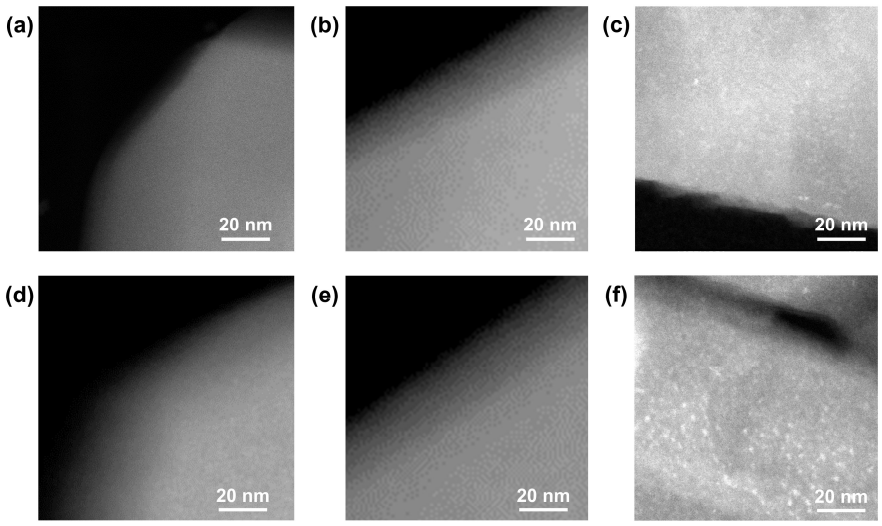

Figure S8 HAADF-STEM images of sulfided and regenerated ZnO@silicalite-1 with different ZnO loadings.

(a)-(c) HAADF-STEM images of sulfided 1 wt% ZnO@silicalite-1, 2 wt% ZnO@silicalite-1 and 5 wt% ZnO@silicalite-1, respectively. (d)-(f) HAADF-STEM images of regenerated 1 wt% ZnO@silicalite-1, 2 wt% ZnO@silicalite-1 and 5 wt% ZnO@silicalite-1 after 4 sulfidation-regeneration cycles, respectively.

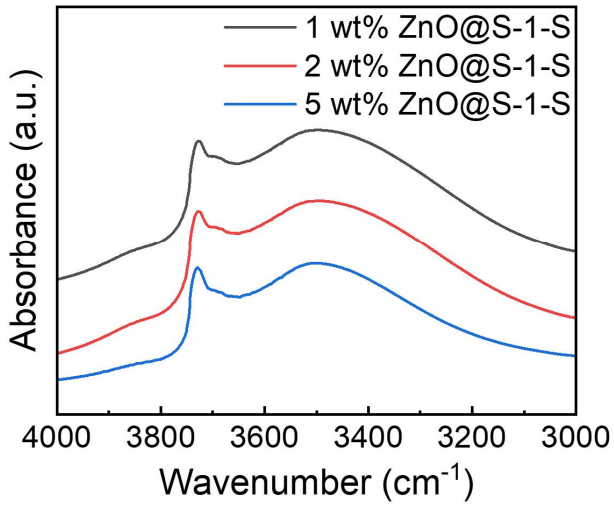

Figure S9 DRIFT spectra of sulfided ZnO@silicalite-1 with different ZnO loadings

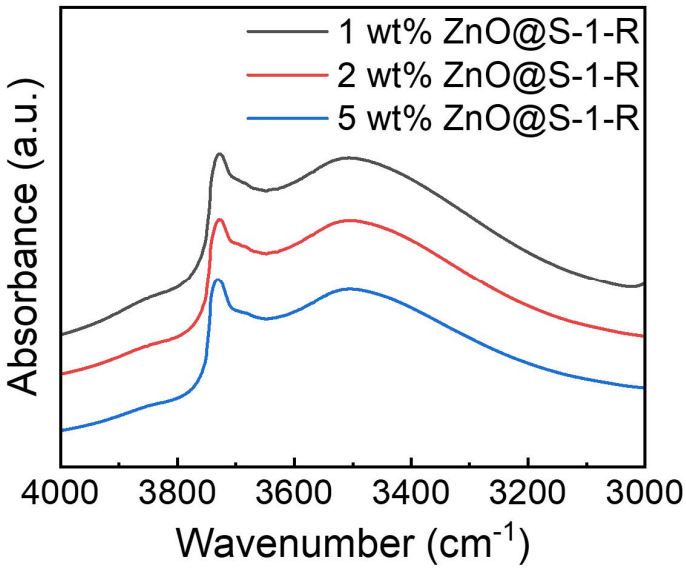

Figure S10 DRIFT spectra of regenerated ZnO@silicalite-1 with different ZnO loadings after 4 cycles

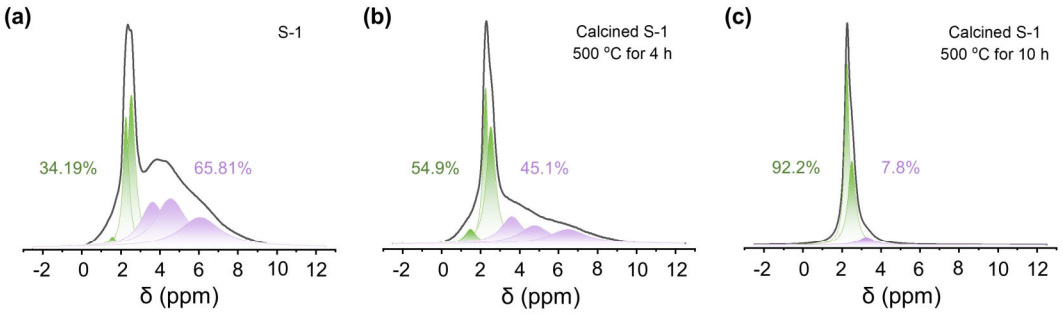

Figure S11 ^{1}H MAS NMR spectra of silicalite-1 zeolite after different calcination conditions.

(a) ^{1}H MAS NMR spectrum of the silicalite-1 zeolite after the calcination for removing OSDA (the calcination condition was done at 550 °C for 7 h). (b) ^{1}H MAS NMR spectrum of the silicalite-1 zeolite after a second-step calcination at 500 °C for 4 h. (c) ^{1}H MAS NMR spectrum of the silicalite-1 zeolite after a second-step calcination at 500 °C for 10 h.

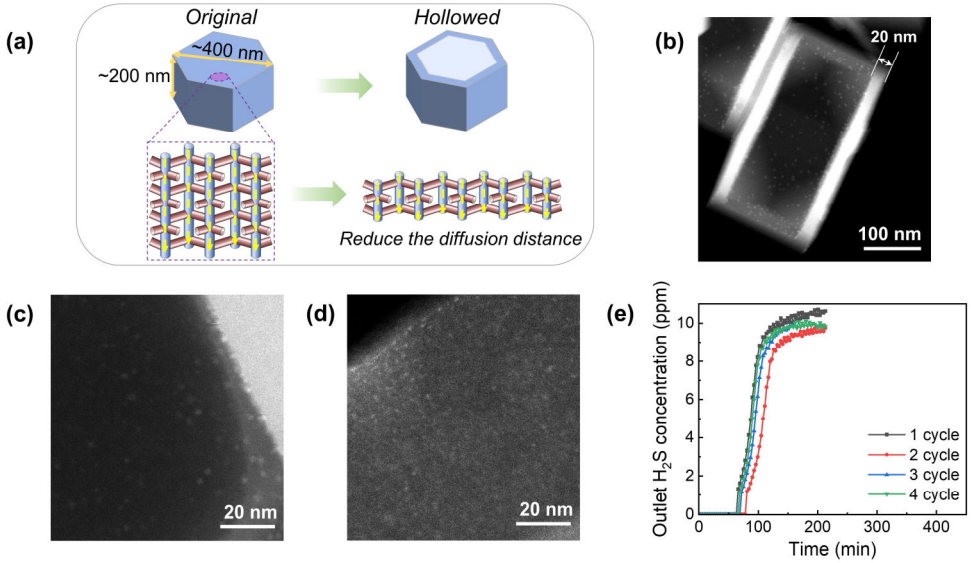

Figure S12 Hollow silicalite-1 (Hol-S-1) adsorbent and its desulfurization performance.

(a) Simplified schematic of hollowing; (b)-(c) HAADF-STEM images of 2% ZnO@ Hol-S-1 with different magnification; (d) HAADF-STEM images of regenerated 2% ZnO@ Hol-S-1 after 4 successive sulfidation-regeneration cycles; (e) H_2S breakthrough curves during consecutive 4 sulfidation-regeneration cycles for 2% ZnO@Hol-S-1. Initial H_2S concentration is 10 ppm, and adsorption and regeneration temperature are 150 °C and 500 °C, respectively.

References

(1) Rehr, J. J.; Kas, J. J.; Vila, F. D.; Prange, M. P.; Jorissen, K. Parameter-Free Calculations of X-Ray Spectra with FEFF9. *Phys. Chem. Chem. Phys.* **2010**, *12* (21), 5503–5513.

(2) Protsak, I. S.; Morozov, Y. M.; Dong, W.; Le, Z.; Zhang, D.; Henderson, I. M. A 29Si, 1H, and 13C Solid-State NMR Study on the Surface Species of Various Depolymerized Organosiloxanes at Silica Surface. *Nanoscale Res Lett* **2019**, *14* (1), 160.

(3) Trzpit, M.; Rigolet, S.; Paillaud, J.-L.; Marichal, C.; Soulard, M.; Patarin, J. Pure Silica Chabazite Molecular Spring: A Structural Study on Water Intrusion−Extrusion Processes. *J. Phys. Chem. B* **2008**, *112* (24), 7257–7266.

(4) d'espinose de la Caillerie, J.-B.; Aimeur, M. R.; Kortobi, Y. E.; Legrand, A. P. Water Adsorption on Pyrogenic Silica Followed by1H MAS NMR. *Journal of Colloid and Interface Science* **1997**, *194* (2), 434–439.

(5) Qin, Z.; Lakiss, L.; Tosheva, L.; Gilson, J.-P.; Vicente, A.; Fernandez, C.; Valtchev, V. Comparative Study of Nano-ZSM-5 Catalysts Synthesized in OH− and F− Media. *Advanced Functional Materials* **2014**, *24* (2), 257–264.

(6) Dib, E.; Costa, I. M.; Vayssilov, G. N.; Aleksandrov, H. A.; Mintova, S. Complex H-Bonded Silanol Network in Zeolites Revealed by IR and NMR Spectroscopy Combined with DFT Calculations. *J. Mater. Chem. A* **2021**, *9* (48), 27347–27352.

(7) Hunger, M.; Ernst, S.; Steuernagel, S.; Weitkamp, J. High-Field 1H MAS NMR Investigations of Acidic and Non-Acidic Hydroxyl Groups in Zeolites H-Beta, H-ZSM-5, H-ZSM-58 and H-MCM-22. *Microporous Materials* **1996**, *6* (5), 349–353.